Rapid visible-light degradation of malachite green enabled by nanorod cobalt hydroxycarbonate: performance and mechanisms

Jing Guo*, Rui Wu, Qi Wang, Xiaomei Zhao, Jinlei Yang, Jinping Sha

Ningxia Key Laboratory of Green Catalytic Materials and Technology, College of Chemistry and Chemical Engineering, Ningxia Normal University, Guyuan 756099, China

Address correspondence to E-mail: guojingsn@163.com

1 Experiment

1.1 Materials

Cobalt(II) chloride hexahydrate ($CoCl_2 \cdot 6H_2O$), Cobalt(II) nitrate hexahydrate ($Co(NO_3)_2 \cdot 6H_2O$), Urea ($CO(NH_2)_2$), and Malachite Green (MG) were bought from Aladdin Reagent Biochemical Technology Co., Ldt (Shanghai, China). Ethylene glycol (EG), and ethanol (C_2H_5OH) were bought from Sinopharm Chemical Reagent Co., Ldt (Shanghai, China). Tert-butyl alcohol (TBA, $C_4H_{10}O$), ascorbic acid (VC, $C_6H_8O_6$), peroxymonosulfate (PMS, $KHSO_5 \cdot 0.5KHSO_4 \cdot 0.5K_2SO_4$), ethylenediaminetetraacetic acid (EDTA-2Na, $C_{10}H_{14}N_2Na_2O_8$), and L-histidine (L-His, $C_6H_9N_3O_2$) were from Maclin Biochemical Technology Co., Ldt (Shanghai, China). Additionally, sodium nitrate ($NaNO_3$), sodium sulfate (Na_2SO_4), sodium dihydrogen phosphate (NaH_2PO_4), disodium hydrogen phosphate (Na_2HPO_4), sodium oxalate ($Na_2C_2O_4$), methanol (MeOH, CH_4O) was provided by Lianlong Bohua Tianjin Pharmaceutical Chemical Co., Ltd. All the obtained reagents were of pure analytical grade and were used for direct use without additional purification. Deionized water was RO water from a laboratory water purification system.

1.2 Characterization

Crystal structure of the samples was characterized by X-ray diffraction (XRD, Rigaku D/MAX 2500V, Japan) using Cu Kα radiation (λ = 1.5406 Å) operated at 40 kV and 50 mA, with data collected in the 2θ range of 5–90° at a step size of 0.02° and a scanning speed of 2 °/min. Morphological and structural features were examined by field emission scanning electron microscopy (FE-SEM, ZEISS Sigma 300, Germany) and transmission electron microscopy (TEM, JEOL JEM-F200, Japan); chemical composition and elemental valence states were analyzed by X-ray photoelectron spectroscopy (XPS, Thermo Scientific K-Alpha, USA). Fourier transform infrared (FT-IR) spectra were recorded on a Nicolet 6700 spectrometer to identify functional groups and chemical bonds. The concentration of MG during the photocatalytic process was monitored using a UV–Vis spectrophotometer (P4, MAPADA, Shanghai). Specific surface area was determined by nitrogen adsorption–desorption measurements at 77 K on a Micromeritics 3020 analyzer, and the Bruner–Emmett–Teller (BET) method was

applied for calculation. The leaching of cobalt ions from the solution was analyzed using inductively coupled plasma-optical emission spectrometer (ICP-OES, Agilent 5110).

1.3 Analytical methods

Degradation intermediates were analyzed using the chromatographic column Waters BEH C18 (2.1 × 100 mm, 1.7 um) in combination with a high-performance liquid chromatography-mass spectroscopy (HPLC-MS) system. A formic acid aqueous solution (0.1%) was used as the mobile phase A, and an acetonitrile solution was used as the mobile phase B; the flow rate was set at 0.3 $mL \cdot min^{-1}$. The injection volume of the liquid was 5 μL, and the scanning range was controlled from 50 to 1000 m/z. The sheath gas temperature and flow were set at 350℃ and 12 $L \cdot min^{-1}$, respectively.

1.4 Measurement of photocatalytic activity

The photocatalytic performance of the synthesized samples was evaluated by Malachite Green (MG, 50 mL, 50 $mg \cdot L^{-1}$) under visible-light irradiation ($\lambda > 420$ nm) from a 300 W xenon lamp. Prior to irradiation, the suspension was magnetically stirred in the dark for 30 min to establish adsorption–desorption equilibrium. During the irradiation process, approximately 3 mL of the suspension was sampled at regular intervals and immediately filtered through a 0.22 μm polytetrafluoroethylene membrane. Concentration of MG in the filtrate was determined by UV–Vis spectroscopy. Degradation efficiency (R) was calculated using the following equation: R (%) = $((C_0\text{-}C_t)/C_0) \times 100\%$, where C_0 denotes the concentration of pollutants in the initial sample, and C_t represents the concentration in the sample after photodegradation, measured at a given sampling[1-3].

2 Results and Discussions

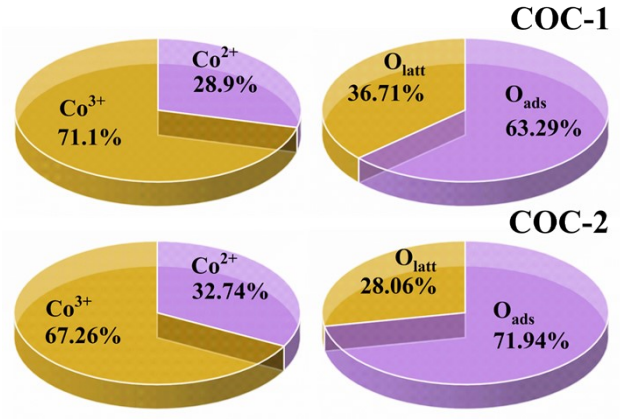

Fig. S1 Fractions of Co and O species in COC-1 and COC-2.

Table S1 S_{BET}, pore volume and pore size of the prepared samples

Samples	S_{BET} ($m^2 \cdot g^{-1}$)	V_p ($cm^3 \cdot g^{-1}$)	Pore Diameter (nm)
COC-1	32.4	0.089	12.191
COC-2	3.3	0.013	15.478

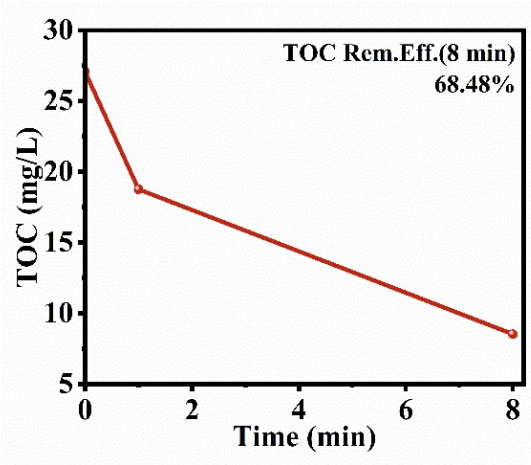

Fig. S2 mineralization rate measured at 8 min.

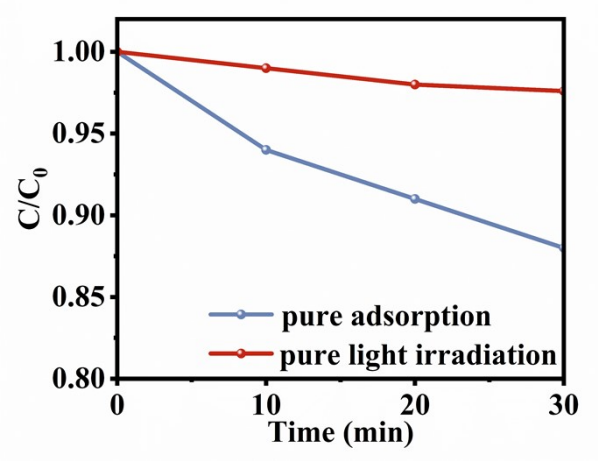

Fig. S3 Pure adsorption and pure light irradiation for 30 min.

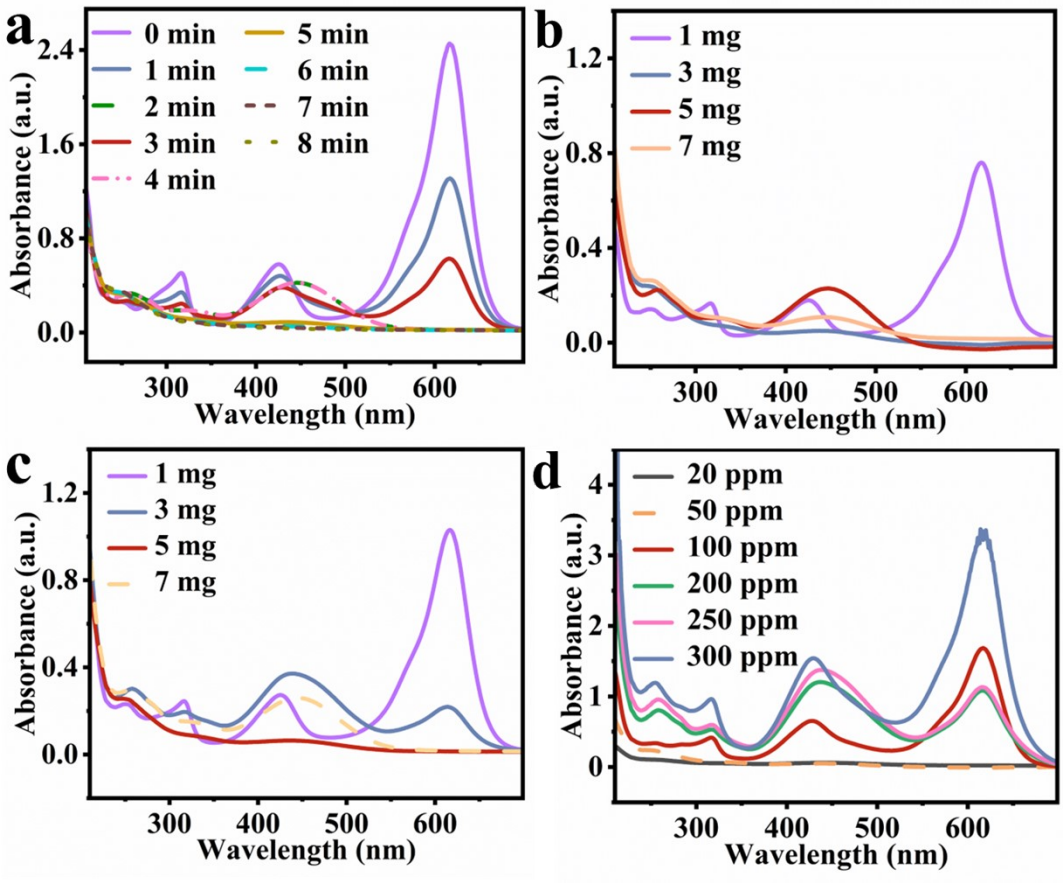

Fig. S4 UV-Vis absorption spectra of MG solutions under different reaction conditions: **a** COC-2, **b** Cat. dosage, **c** PMS dosage and **d** MG concentration.

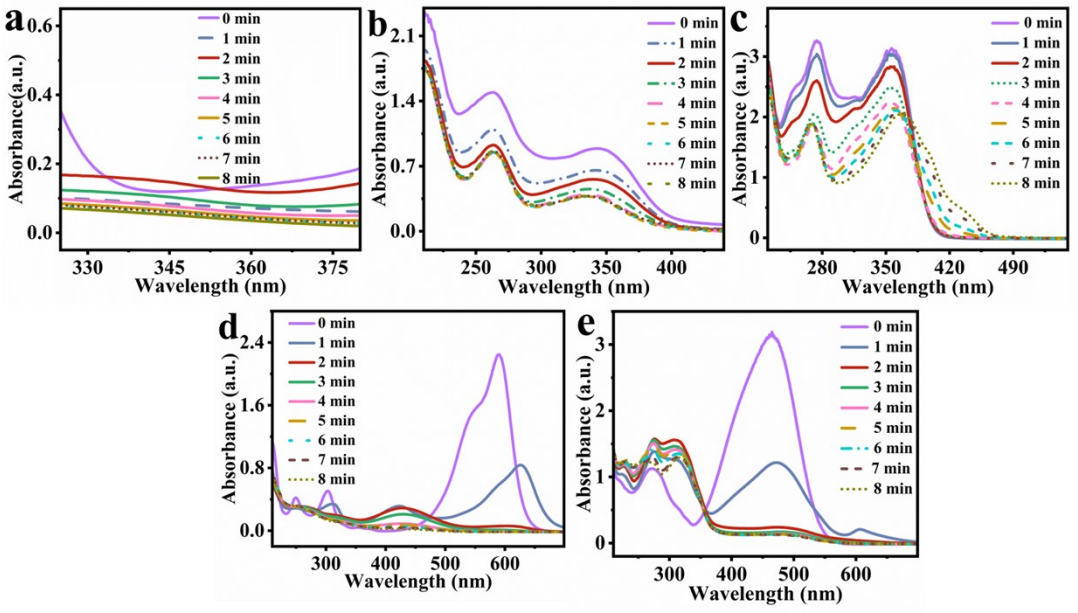

Fig. S5 UV-Vis absorption spectra for **a** MG (320-380 nm); **b** OTC, **c** TC-HCl, **d** CV, and **e** MO degradation under light irradiation.

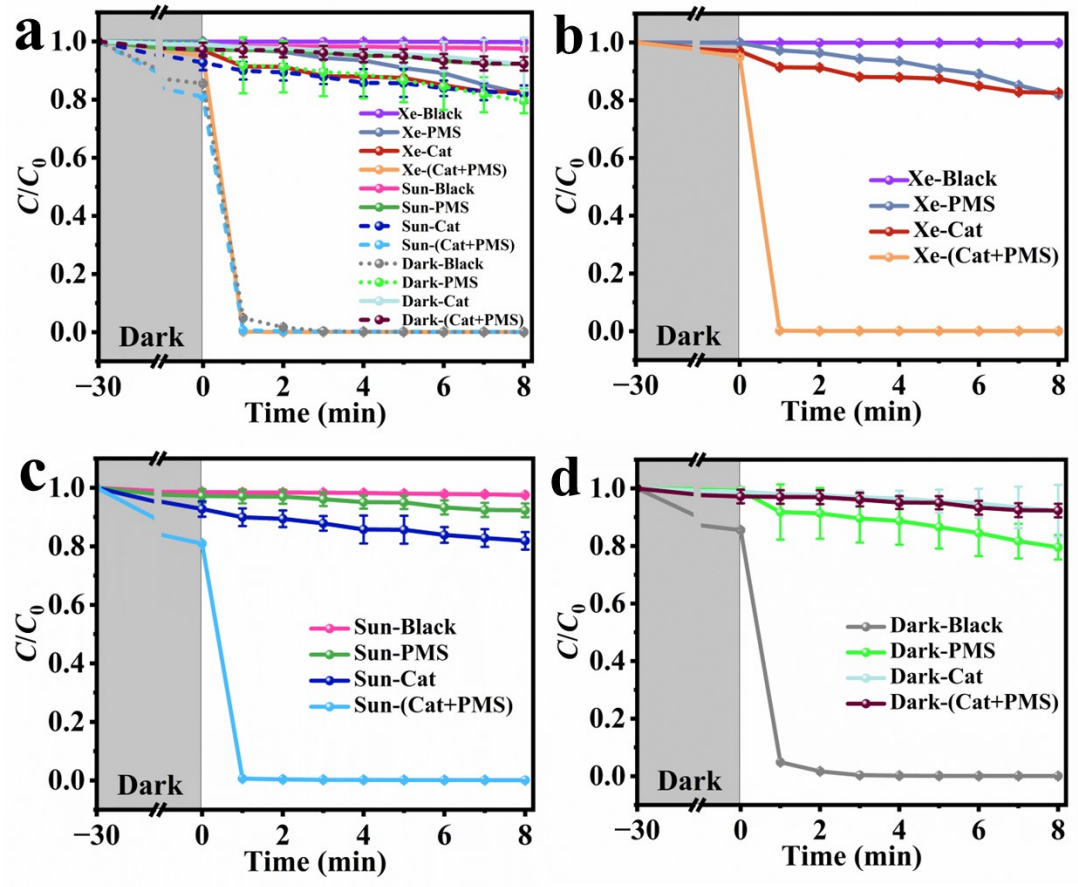

Fig. S6 Effect of light source on MG degradation activity: **a** different light sources (comparison), **b** visible light, **c** sunlight, and **d** dark condition.

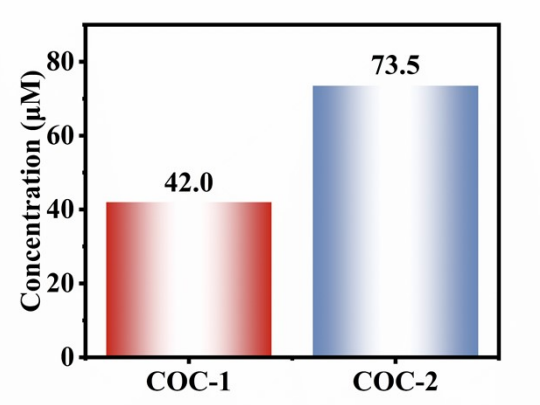

Fig. S7 Metal ion leaching of COC-1 and COC-2.

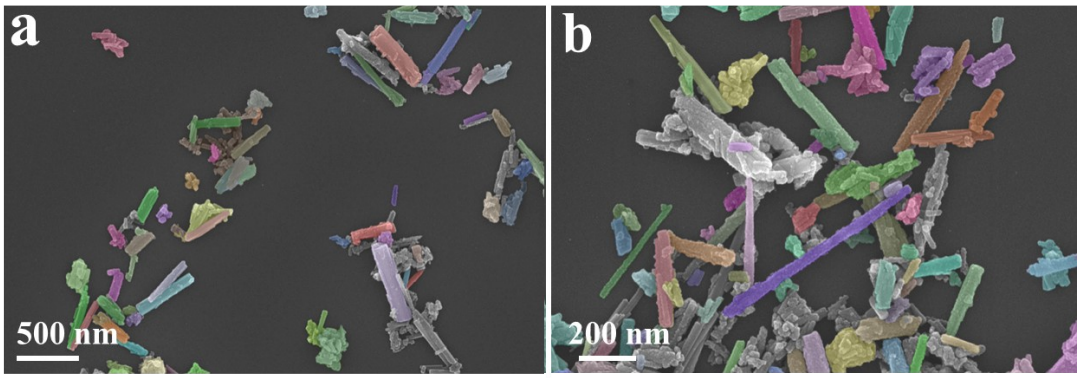

Fig. S8 SEM images of COC-1 after five cycles.

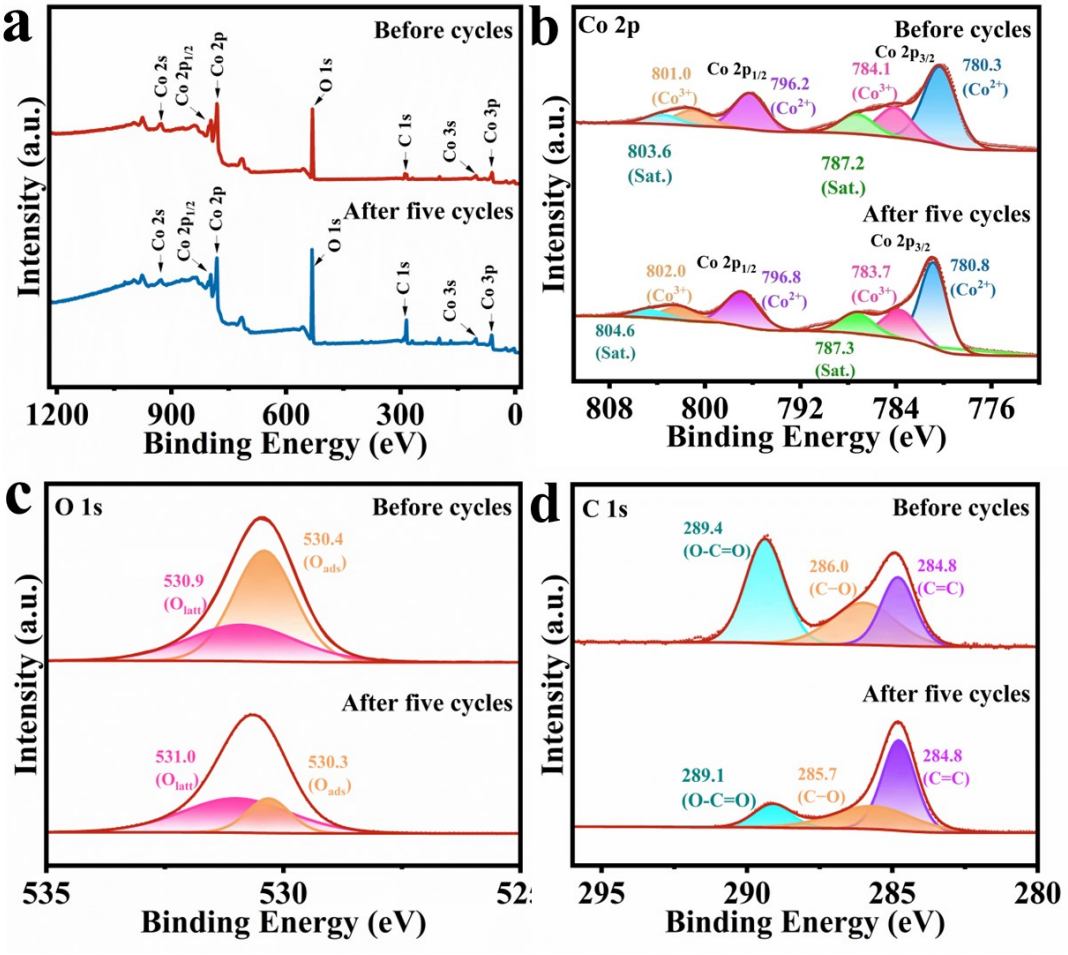

Fig. S9 XPS spectra of COC-1 after five cycles: **a** survey spectrum, **b** Co 2p, **c** O 1s, and **d** C 1s.

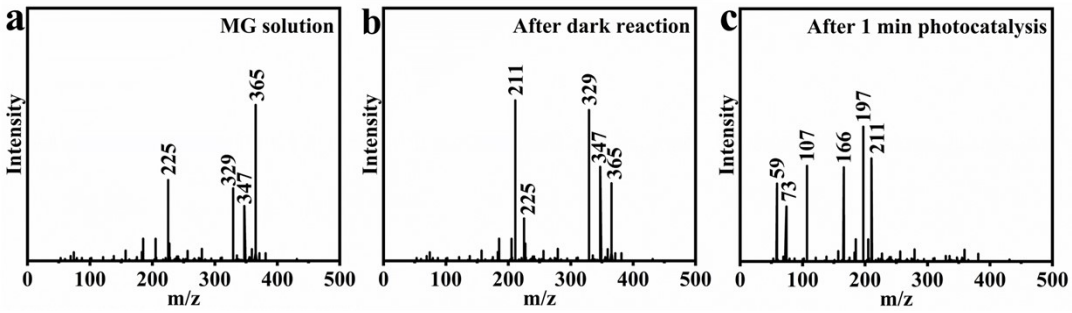

Fig. S10 HPLC-MS spectra of the solution samples during the MG degradation.

Table S2 Identification of MG for COC-1 degradation intermediates by HPLC-MS

Compound	Structure	Formula	m/z
	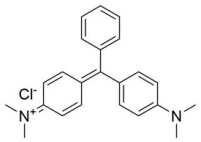	$C_{23}H_{25}ClN_2$	365
P1	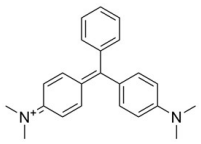	$C_{23}H_{25}N_2^+$	329
P2	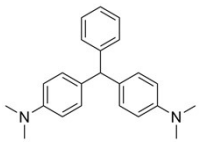	$C_{23}H_{26}N_2$	330
P3	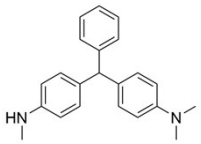	$C_{22}H_{24}N_2$	315
P4	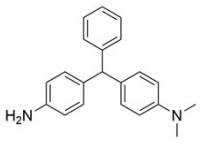	$C_{21}H_{22}N_2$	301
P5	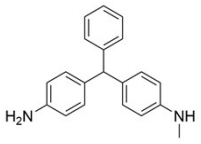	$C_{20}H_{20}N_2$	287
P6	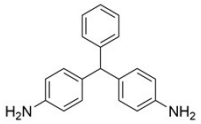	$C_{19}H_{18}N_2$	273
P7	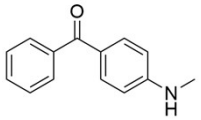	$C_{15}H_{15}NO$	215
P8	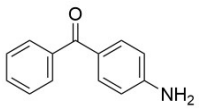	$C_{13}H_{11}NO$	197
P9	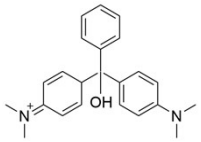	$C_{24}H_{28}N_2O^+$	347
P10	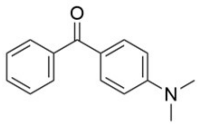	$C_{15}H_{15}NO$	225

P11	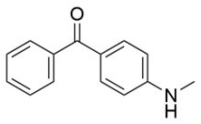	$C_{14}H_{13}NO$	211
P12	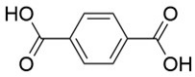	$C_8H_6O_4$	166
P13	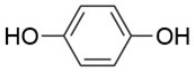	$C_6H_6O_2$	110
P14	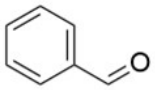	C_7H_6O	107
P15	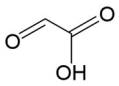	$C_2H_2O_3$	73
P16	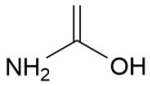	C_2H_5NO	59

Reference

1. F. Qiu, Y. Pan, L. Wang, H. Song, X. Liu, Y. Fan and S. Zhang, *Sep. Purif. Technol.*, 2024, **330**, 125139.
2. H. Salehzadeh, M.J. Rezaei, B. Shahmoradi, B. Nikkhoo, A. Allahweisi, A. Maleki, B. Rahimi, M. Rezaee, K. Nasiri and H.-J. Choi, *J. Environ. Manage.*, 2025, **386**, 125710.
3. L.R. Jabbar, S.H. Ammar and A.A. Amooey, *J. Water Process. Eng.*, 2025, **77**, 108545.